iScience, Volume *25*

Supplemental information

A parasite outbreak in notothenioid fish in an Antarctic fjord

Thomas Desvignes, Henrik Lauridsen, Alejandro Valdivieso, Rafaela S. Fontenele, Simona Kraberger, Katrina N. Murray, Nathalie R. Le François, H. William Detrich III, Michael L. Kent, Arvind Varsani, and John H. Postlethwait

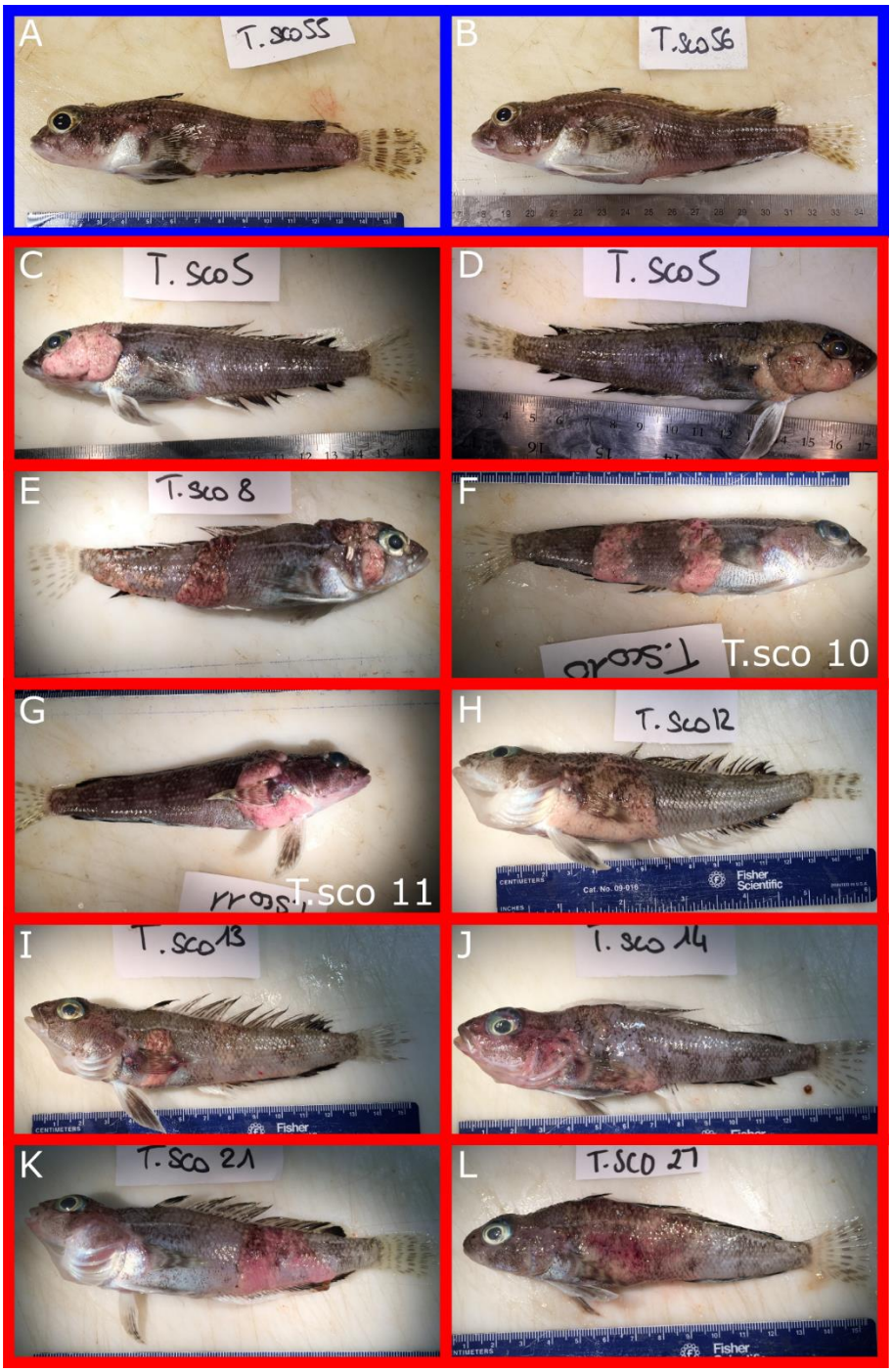

Figure S1. Examples of tumors in crowned notothens *Trematomus scotti*, related to Figure 1. (A-B) Specimens framed in blue are apparently healthy fish. (C-L) Specimens framed in red represent a diversity of pathological manifestations of X-cell xenomas. The label "T.sco#" refers to the specimen field identification code.

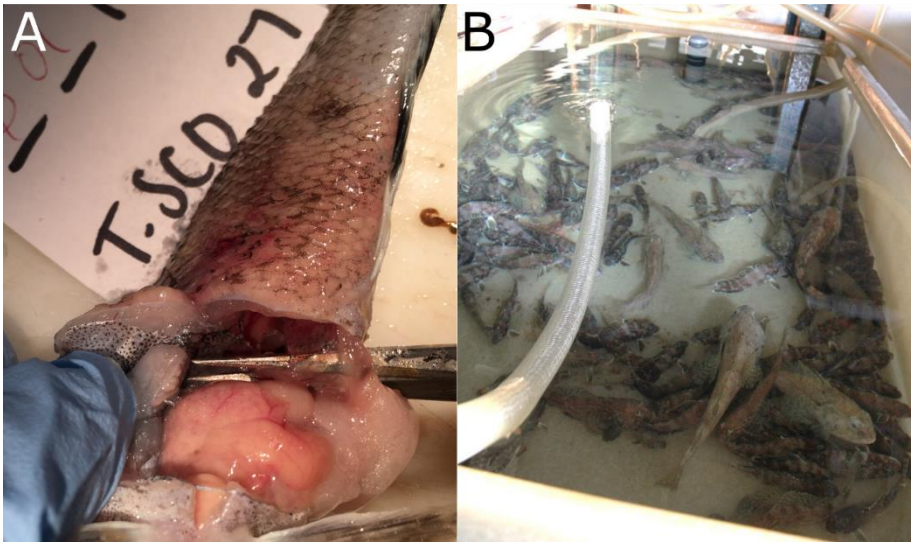

Figure S2. Dissection of diseased *Trematomus scotti* in 2018 and catch from Andvord Bay in April 2014, related to Figure 1. (A) Dissection of diseased *Trematomus scotti* suggested the tumors remained superficial and did not invade underlying tissue and the body cavity. (B) Palmer Station holding tank containing many *T. scotti* (along with a few *Trematomus bernacchii*, *Trematomus hansoni* and *Gobionotothen gibberifrons*) captured at the same location in Andvord Bay in April 2014. None of the specimens in this picture or others observed at the time displayed lesions similar to those observed in 2018.

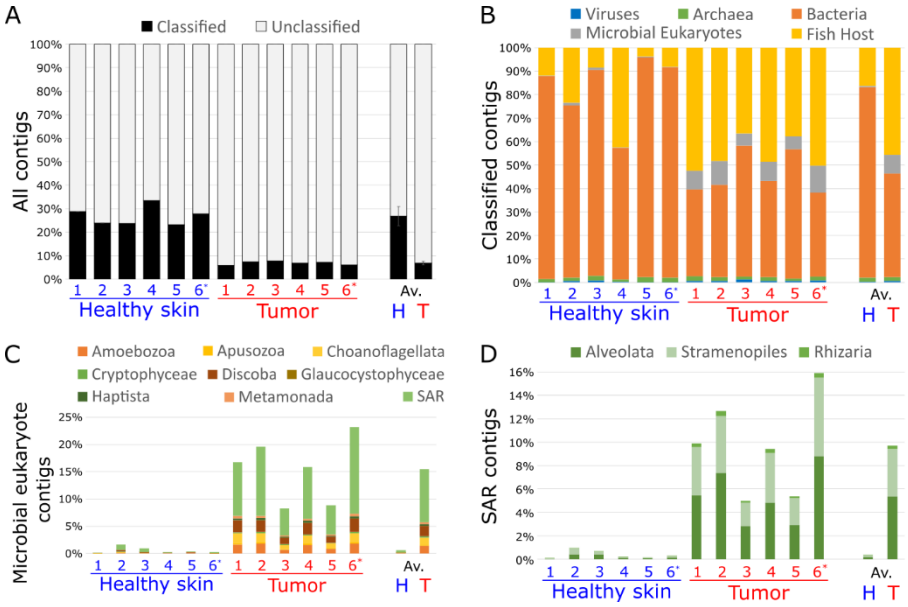

Figure S3. Metagenomic analyses of healthy skin and tumor samples, related to Figure 2A-C. Blue and red denote healthy skin (H) and tumor (T) samples, respectively. Asterisks (*) denote samples from *Nototheniops larseni* (A) Proportions of contigs taxonomically classified and unclassified by Kaiju software. (B) Proportions of classified contigs including fish contigs. (C) Proportions of microbial eukaryote contigs by group. (D) Proportions of SAR contigs by group. The Alveolata group is moderately enriched over Stramenopiles and Rhizaria groups. Av., average across biological replicates.

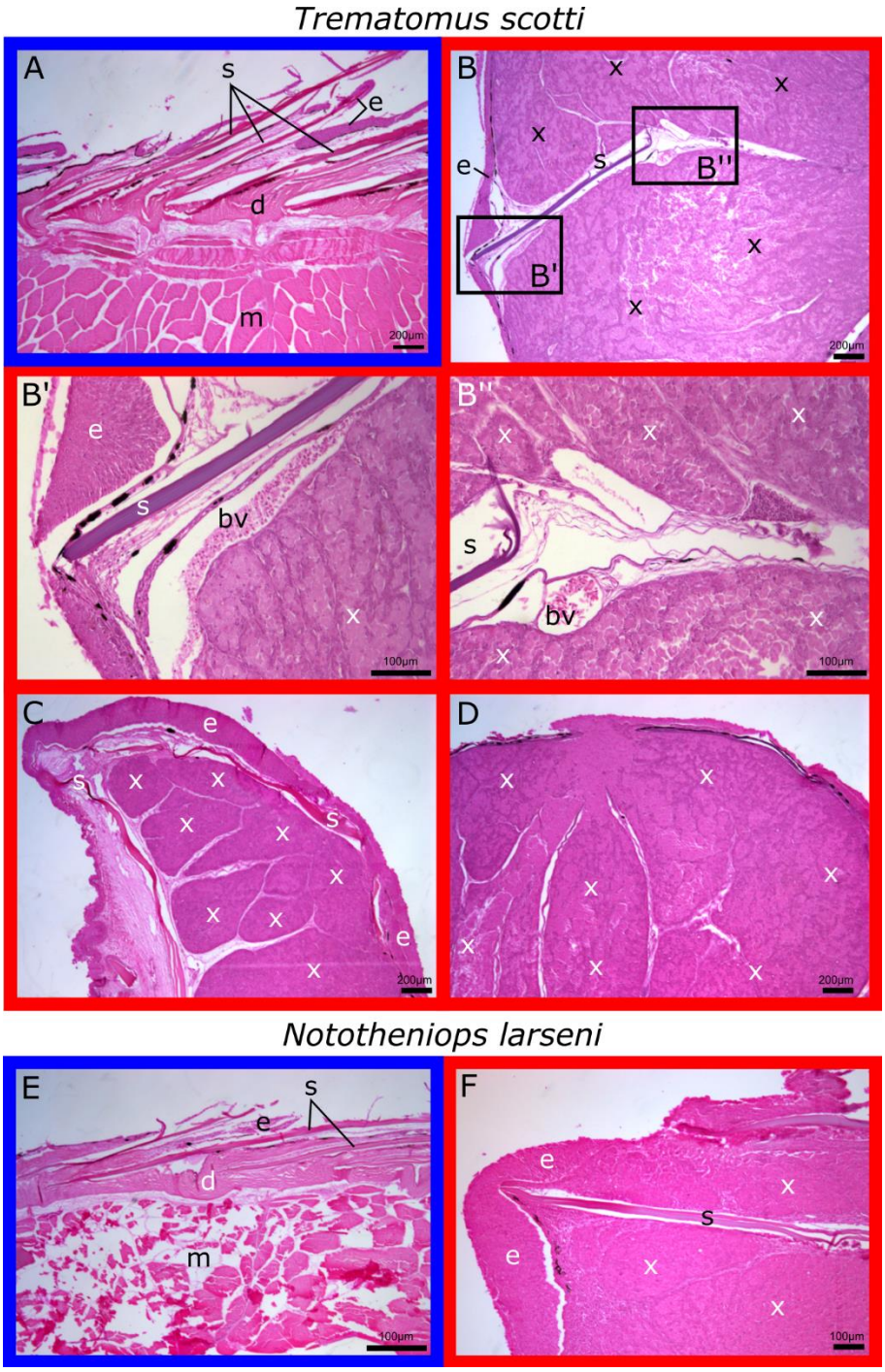

Figure S4. Histopathology of X-cell xenomas in *Trematomus scotti* and *Nototheniops larseni*, related to Figure 2D-F. Histopathology of xenomas (A-D) in *Trematomus scotti* and (E-F) in *Nototheniops larseni*. Micrographs framed in blue (A, E) are examples of healthy skins and micrographs framed in red (B-D, F) illustrate diverse features of X-cell xenomas. Abbreviations: bv, blood vessel; d, dermis; e, epidermis; m, muscle; s, scale; x, xenomas.

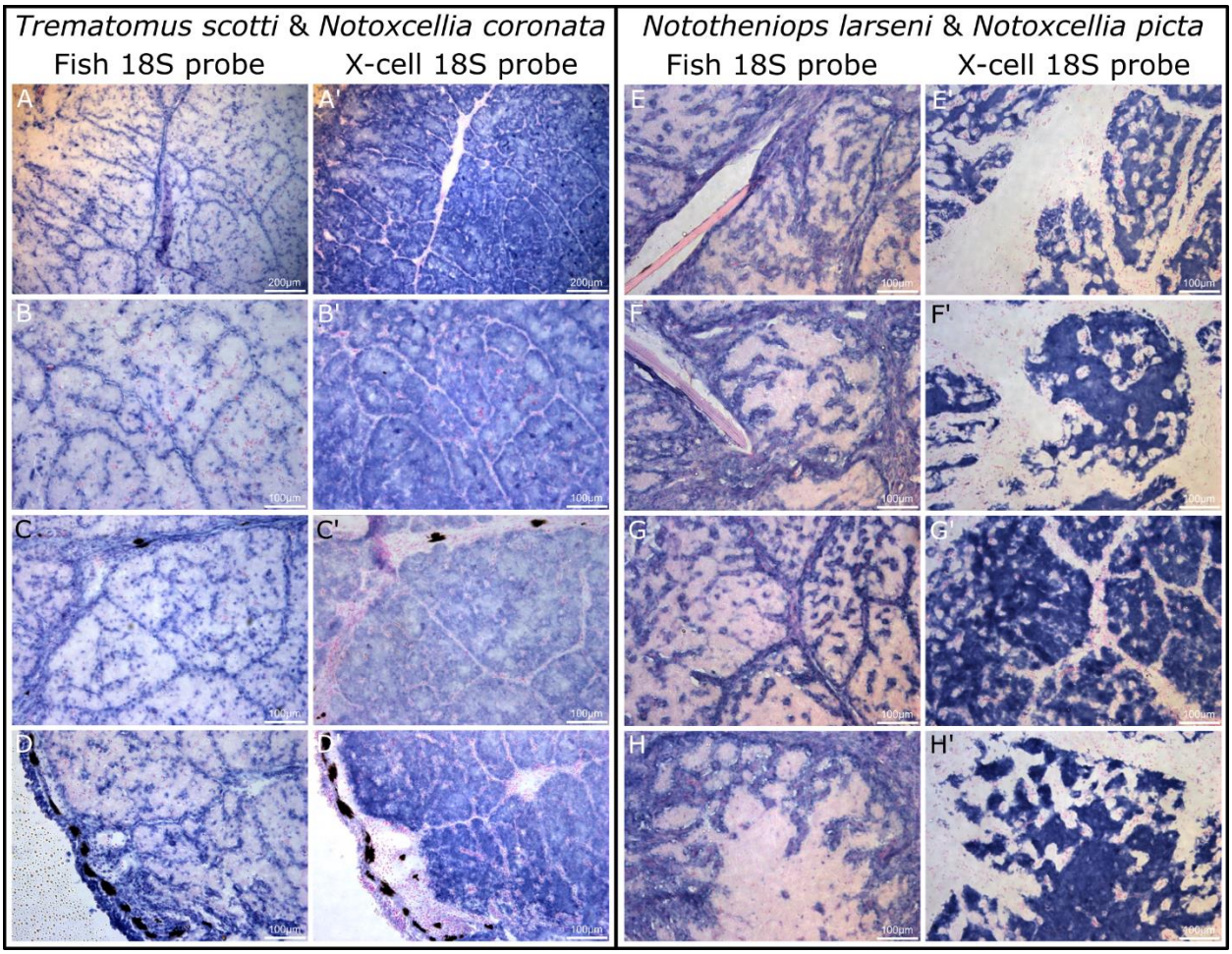

Figure S5. *In situ* hybridization of *Notoxcellia coronata* and host fish *Trematomus scotti* 18S SSU rRNA and of *Notoxcellia picta* and host fish *Nototheniops larseni* in alternate sections of tumor xenomas, related to Figure 2I-K. *In situ* hybridization was carried out on adjacent cryosections using (A-H) a probe against the host fish 18S SSU rRNA (A-D, *Trematomus scotti*; E-H, *Nototheniops larseni*) and (A'-H') with a probe against X-cell 18S SSU rRNA (A'-D', *Notoxcellia coronata*; E'-H', *Notoxcellia picta*). Cells positive for each probe are stained blue. Slides were counter-stained with Nuclear Fast Red. Note that X-cell nuclei do not stain well with Nuclear Fast Red.

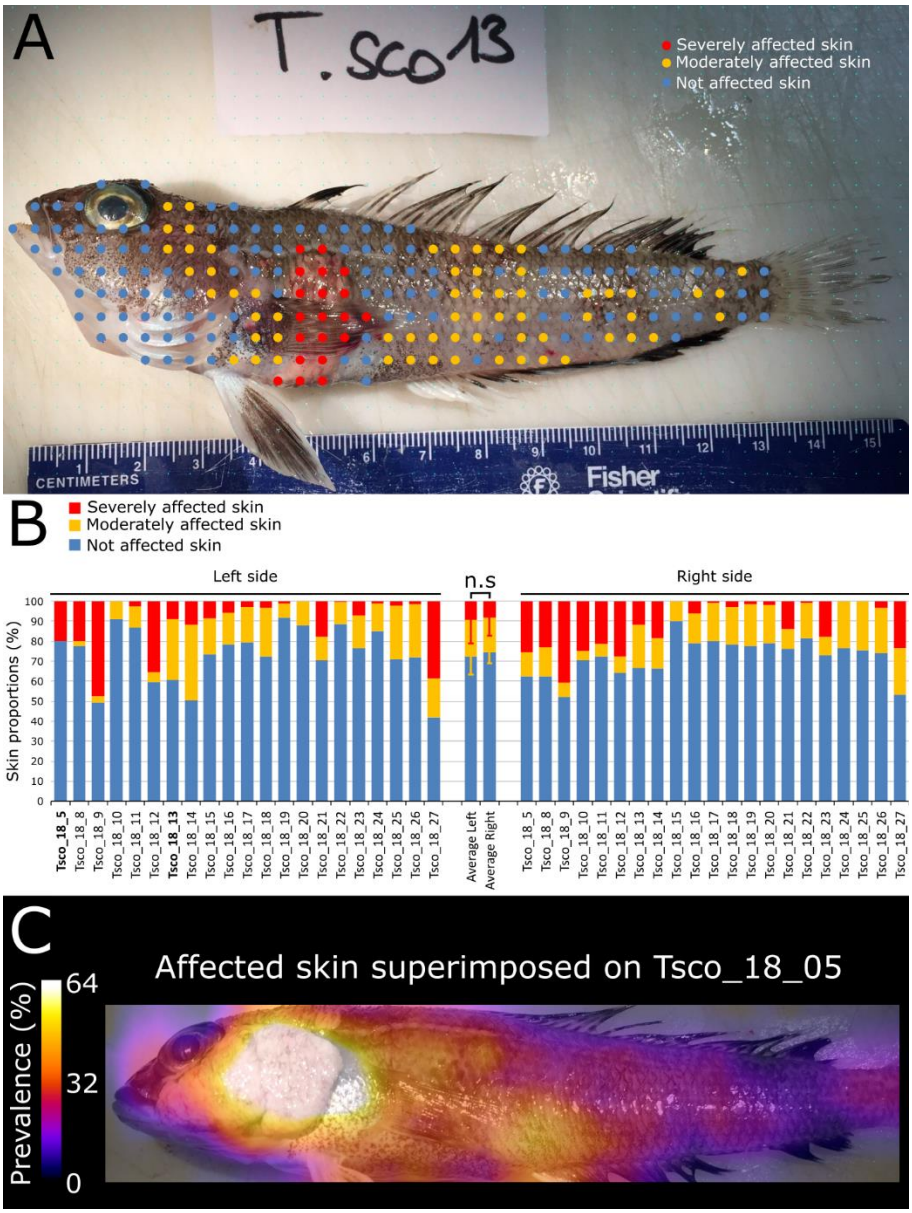

Figure S6. Skin pathology of X-cell infection in *Trematomus scotti*, related to Figure 4A-B. (A) Example of categorization of skin as healthy, moderately affected, or severely affected on the left side of Tsco_18_13 using randomized point grid. (B) Proportions of skin conditions on the left and right sides of all 21 out of 24 studied crowned notothens. Averages for each side are presented in the middle of the panel. Left and right sides were not significantly different in infection ($p = 0.52$, n.s, not significant). The left side images of the *Trematomus scotti* specimens used in (A) and (C) are indicated in bold in B. (C) Prevalence map of X-cell infection on the body of 21 crowned notothens superimposed on Tsco_18_05.

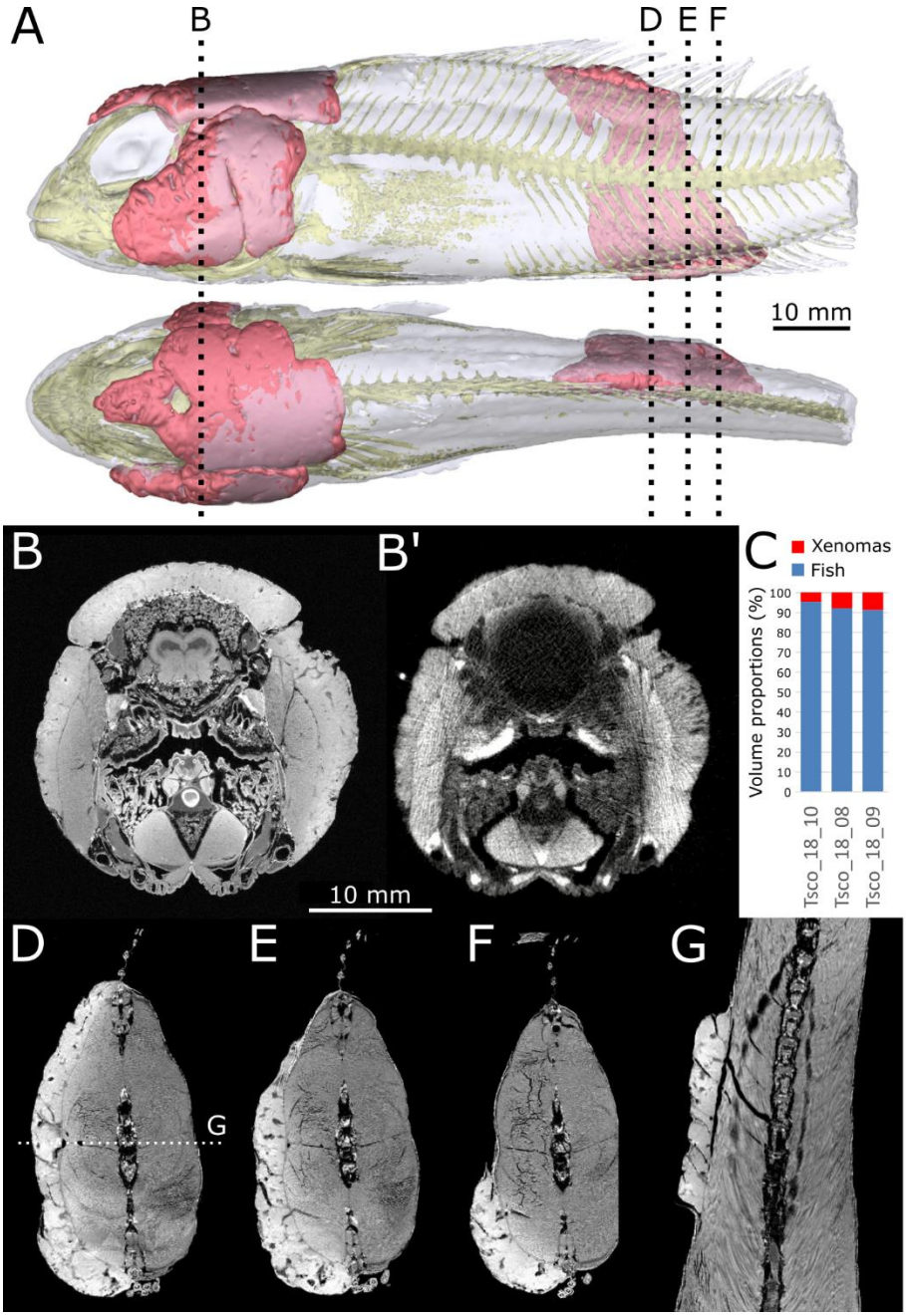

Figure S7. *Trematomus scotti* microCT and microMRI analyses, related to Figure 4C-J. (A) Crowned notothen Tsco_18_08 analyzed by microMRI and resulting segmented 3D model in left lateral and dorsal views. The fish skeleton is represented in yellow and the tumors in pink. (B) microMRI and (B') microCT-scan slices through the head as positioned in (A) show the xenomas did not invade internal organs. (C) In the three analyzed specimens, xenomas occupied 4.5 to 8.75 % of the specimen volume. (D-G) Individual microMRI slices as positioned in (A and D) illustrating the enlarged intersegmental blood vessels.

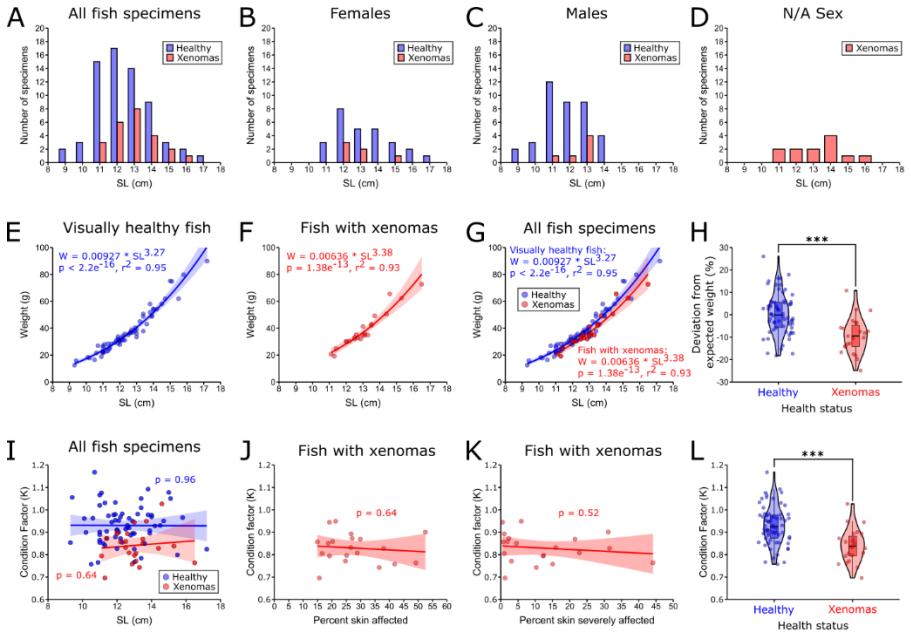

Figure S8. Morphometric analyses of *Trematomus scotti* from Andvord Bay, related to Figure 4K-M. Size distribution (standard length, SL) of (A) all studied *Trematomus scotti* specimens, (B) female, (C) male, and (D) sexually undetermined (N/A) individuals. Growth models of (E) visually healthy fish, (F) fish with xenomas, and (G) both models of visually healthy fish and fish with xenomas. (H) Deviation from expected weight in fish with xenomas compared to visually healthy fish (%). Fish with xenomas are on average 10% lighter than their expected weight based on their SL (one-sided t-test, t = 4.73, df = 43.2, p = 1.22e-5). The Fulton's condition factor K is not correlated to (I) the SL in both healthy fish and fish with xenomas, (J) the percentage of skin affected (moderately + severely affected), or (K) the percentage of severely affected skin in fish with xenomas, which allows the study of the effect of xenomas as a binary variable (presence/absence) independent of fish SL or percentage of skin affected. (L) Fish with xenomas have a lower condition factor K than visually healthy fish (one-sided t-test, t = 4.73, df = 43.2, p = 1.22e-5).

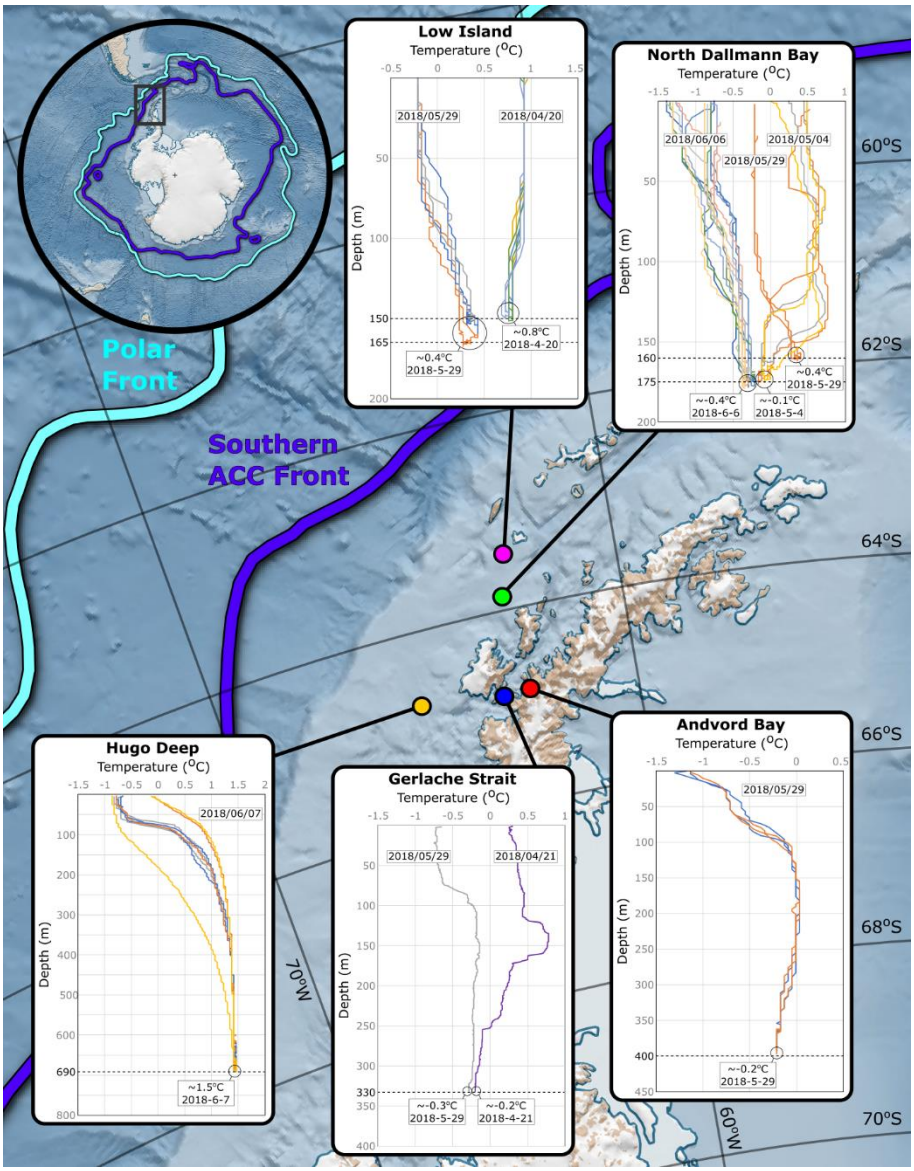

Figure S9. Temperature profiles along the West Antarctic Peninsula, related to Figure 1. Temperature profiles in degree Celsius (ºC) at five fishing locations on the West Antarctic Peninsula during austral fall 2018. Most profiles were recorded using a DST centi-TD Miniature Temperature and Depth Data Logger (Star-Oddi, Garðabær, Iceland) mounted on one of the two otter doors of the trawl, thus providing a continuous temperature record as the net descended during deployment, rode the bottom, and ascended during retrieval. The two temperature profiles in the Gerlache Strait were recorded using XBT probes (Expendable Bathythermograph) Sippican Deep Blue 760-M and thus show unidirectional temperature profiles.